

# Heterodyne interferometric polarization coherent anti-Stokes Raman scattering (HIP-CARS) spectroscopy

K. Orsel,<sup>a</sup> E. T. Garbacik,<sup>a</sup> M. Jurna,<sup>a</sup> J. P. Kortrijk,<sup>a</sup> C. Otto,<sup>b</sup> J. L. Herek<sup>a</sup> and H. L. Offerhaus<sup>a\*</sup>

**We demonstrate a new technique that combines polarization sensitivity of the coherent anti-Stokes Raman scattering (CARS) response with heterodyne amplification for background-free detection of CARS signals. In this heterodyne interferometric polarization CARS (HIP-CARS), the major drawbacks of polarization and heterodyne CARS are rectified. Using a home-built picosecond optical parametric oscillator, we are able to address vibrational stretches between 600 and 1650  $\text{cm}^{-1}$  and record continuous high-resolution Raman equivalent HIP-CARS spectra. Copyright © 2010 John Wiley & Sons, Ltd.**

**Keywords:** coherent anti-Stokes Raman scattering; nonlinear spectroscopy; heterodyne; polarization; interference

## Introduction

Although first discovered in 1965,<sup>[1]</sup> coherent anti-Stokes Raman scattering (CARS) has attracted much attention in the past decade, boosted by the development of stable, tunable near-infrared (NIR) laser sources. It is now well known as a powerful tool for chemically selective microscopy and high-resolution spectroscopy of complex samples in biology<sup>[2]</sup> and pharmacy.<sup>[3]</sup> The combination of two beams, called the pump and Stokes, at frequencies  $\omega_p$  and  $\omega_s$ , respectively, generates a third beam at the anti-Stokes frequency  $\omega_{as} = 2\omega_p - \omega_s$ . When the difference frequency  $\Omega = \omega_p - \omega_s$  corresponds to a Raman-active vibration in a molecule, a resonant enhancement of the anti-Stokes beam is observed. The signal can be orders of magnitude more intense than that of the spontaneous Raman signal for the same input power.<sup>[4]</sup>

A significant hurdle to the widespread acceptance of narrow-band CARS is the presence of a nonresonant background that can dominate the signal. The removal of this background has been at the core of CARS research, and many techniques have been developed: exploiting the polarization sensitivity (P-CARS)<sup>[5]</sup>; direct analysis of the characteristic CARS spectrum (FM-CARS)<sup>[6]</sup>; using the phase of CARS responses relative to a stable local oscillator (hCARS)<sup>[7,8]</sup>; and recently the use of stimulated Raman scattering.<sup>[9]</sup> However, each of these techniques has its drawbacks, and therefore combinations have been developed that alleviate the drawbacks of one technique with the advantages of another (e.g., HP-CARS).<sup>[10]</sup>

We demonstrate a straightforward and simple method that exploits the synergies between heterodyne amplification and polarization sensitivity of CARS response. This heterodyne interferometric polarization CARS (HIP-CARS) is ideally suited for turnkey CARS systems because it requires minimal realignment and is capable of addressing vibrational stretches in the biologically important fingerprint region (600–1650  $\text{cm}^{-1}$ ) without any interference of the nonresonant background for spectroscopy and microscopy.

## Polarization Sensitivity

An early description of polarization CARS was given by Ahkmanov *et al.* in 1977.<sup>[11]</sup> Consider two input beams at frequencies  $\omega_p$  (pump/probe) and  $\omega_s$  (Stokes) propagating collinear along the z-axis. We define the polarization of the pump beam to lie along the x-axis so that an angle  $\varphi$  separates the pump and Stokes beams (Fig. 1). If the difference frequency between the pump and Stokes waves  $\Omega = \omega_p - \omega_s$  corresponds to a Raman-active resonance of the sample, and if the two-photon transition  $2\omega_p$  is far from the nearest electronic resonance, then we can make the assumption that the nonresonant component of the  $\chi^{(3)}$  tensor is real and shows no preferred direction or depolarization. The resonant and nonresonant contributions to  $\chi^{(3)}$  are then separated in angle. Taking  $\alpha$  as the angle between the polarizations of the pump beam and the nonresonant component of  $\chi^{(3)}$ , it is determined that the ratio of the resonant to nonresonant contributions is maximized when  $\alpha = 45^\circ$ , which occurs when  $\varphi = 71.6^\circ$ .<sup>[12]</sup> The nonresonant component of  $\chi^{(3)}$  is rejected with an orthogonal analyzer (polarizer), leaving only a portion of the differently polarized resonant signal.

## Interferometric Amplification

It has been demonstrated before that the wavelength and phase relations between the various beams involved in the CARS process

\* Correspondence to: H. L. Offerhaus, Optical Sciences group, MESA+ Institute for NanoTechnology, Faculty of Science and Technology (TNW), University of Twente, The Netherlands. E-mail: H.L.Offerhaus@tnw.utwente.nl

a Optical Sciences Group, MESA+ Institute for Nanotechnology, Faculty of Science and Technology (TNW), University of Twente, Enschede, The Netherlands

b Medical Cell Biophysics, MIRA Institute for Biomedical Technology and Technical Medicine, MESA+ Institute for Nanotechnology, Faculty of Science and Technology, University of Twente, The Netherlands

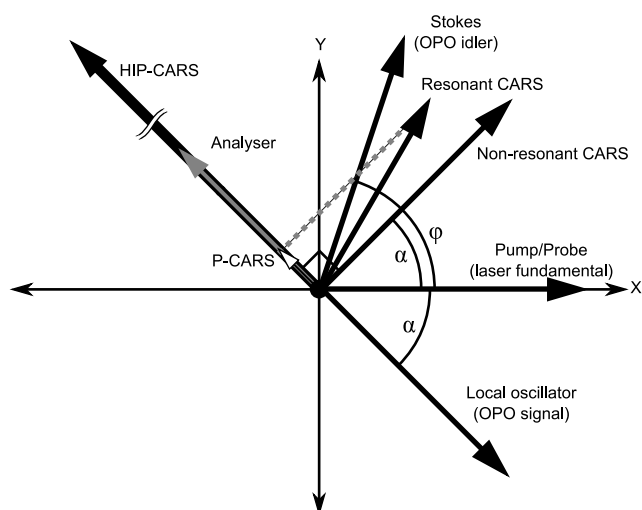


**Figure 1.** Diagram showing the polarizations of various beams. Note that a HIP-CARS beam is not actually created; the vector is intended to convey an enhancement of the P-CARS signal.

allow for interferometric detection.<sup>[13]</sup> The CARS field  $E_{\text{CARS}}$  is combined at the detector with a local oscillator  $E_{\text{LO}}$ . Ignoring a phase offset between the two fields, the detected intensity can be expressed as:

$$I_{\text{detector}} \propto I_{\text{LO}} + I_{\text{CARS}} + 2\sqrt{I_{\text{LO}}I_{\text{CARS}}}\chi_{\text{NR}}^{(3)} + \chi_{\text{R}}^{(3)} \quad (1)$$

where the first two terms represent a DC offset and the third term is an AC signal, provided that either the local oscillator or CARS beam carries a phase modulation. When P-CARS is applied, the nonresonant component will be rejected before the detector by an analyzer, then Eqn 1 reduces to

$$I_{\text{detector}} \propto 2\chi_{\text{R}}^{(3)}\sqrt{I_{\text{LO}}I_{\text{CARS}}} \quad (2)$$

which allows for amplification of the weak CARS beam via interference with a much stronger local oscillator. The main drawback of P-CARS, the loss of a significant portion of the resonant signal, is overcome by the interferometric amplification. The major drawback of heterodyne CARS is that an absolute

phase is required to separate the resonant and nonresonant parts. Because this separation is achieved by the polarization selection in HIP-CARS, there is no need to detect the absolute phase. On the practical side, the heterodyne amplification allows for detection on a photodiode rather than a photomultiplier tube. The photodiode sensitivity extends to longer wavelengths so that IR inputs can be used which is easier on the source and reduces linear absorption and two-photon-induced damage on the sample.

## Experimental

The setup is depicted in Fig. 2. The pump laser is a Coherent Paladin modelocked laser, delivering 12 W at 532 nm and 3 W at 1064 nm at a repetition rate of 80 MHz. We use 530 mW of green laser power to synchronously pump a home-built picosecond optical parametric oscillator (OPO).<sup>[14]</sup> The idler and signal beams generated from this OPO are used as the Stokes and local oscillator waves in the CARS process, respectively, whereas the remainder of the laser fundamental at 1064 nm is used for both the pump and probe waves. The 1064-nm beam is phase modulated by an acoustic optical modulator (AOM) locked to a frequency 50 kHz higher than the laser repetition rate.

Half-wave and quarter-wave plates in all three beams allow precise control of all polarizations to better than  $2^\circ$  and compensate for birefringence induced by the dichroic mirrors. The local oscillator power is attenuated to about 10 nW. The average pump/probe power at the sample is 130 mW, whereas the Stokes power is about 30 mW. The beams are focused into the sample with a Nacet 0.65 NA IR-corrected objective and collected with a long working distance Nikon 0.40 NA objective. The analyzer in this experiment is a polarizing beam cube with an extinction ratio of greater than  $10^4:1$ . Our detector is a ThorLabs SM05PD4B InGaAs photodiode followed by a 10 M $\Omega$  transimpedance amplifier. The amplitude of the modulation on the detected HIP-CARS signal is measured with a Stanford SR570 lock-in amplifier referenced at 100 kHz, twice the frequency shift that the AOM induces on the 1064-nm beam.<sup>[15]</sup> The recorded CARS spectra are processed to account for transmission characteristics of the filters, spectral responses of the detector, and fluctuations in OPO power.

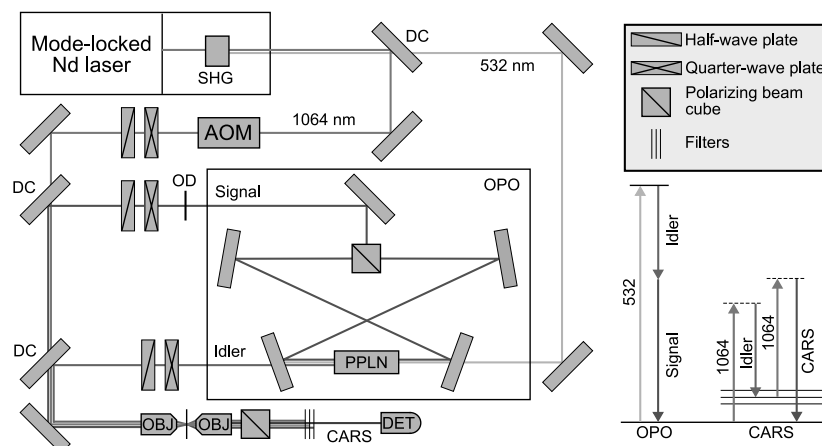


**Figure 2.** Schematic diagram of the setup. SHG, second harmonic generation; DC, dichroic mirror; OD, optical density filter; AOM, acoustic optical modulator; PPLN, periodically poled lithium niobate; OBJ, objective; DET, detector.

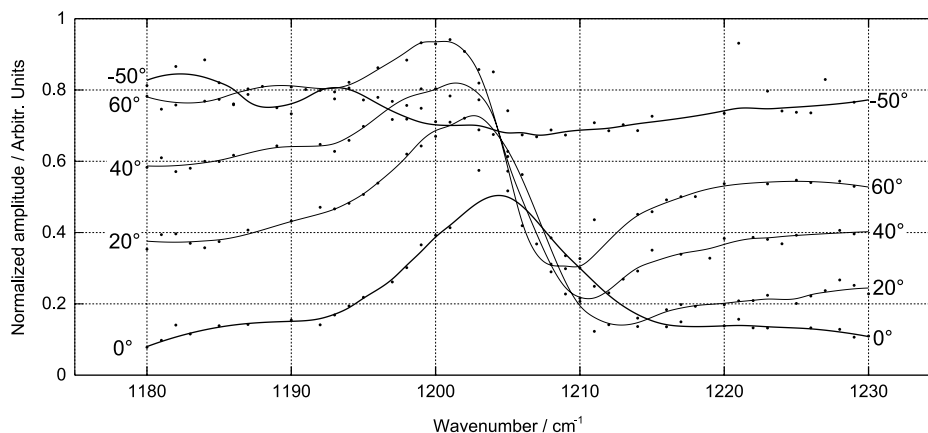


**Figure 3.** HIP-CARS amplitude of toluene around  $1200\text{ cm}^{-1}$  at different angles of the analyzer. Angles are relative to the original P-CARS position of the analyzer (see Fig. 1).

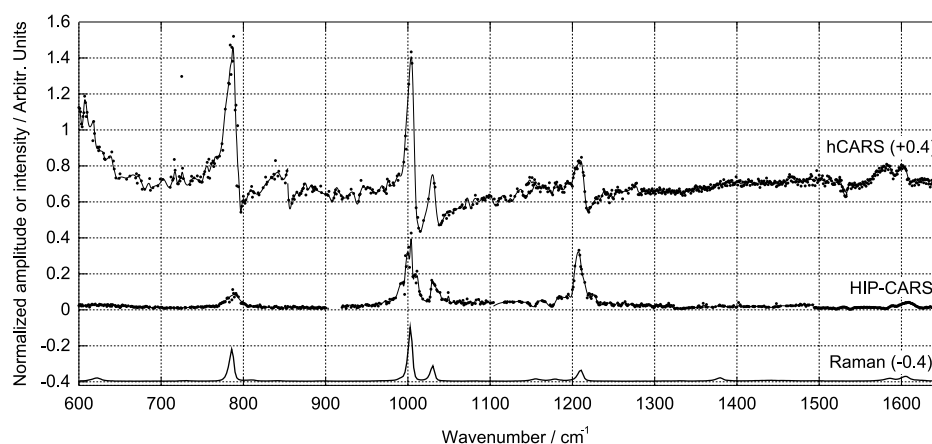


**Figure 4.** HIP-CARS spectrum of toluene (middle) in the fingerprint region. The top line shows the hCARS spectrum, offset by 0.4. The spontaneous Raman spectrum is offset by  $-0.4$ . Because the hCARS and HIP-CARS spectra are taken in several measurements of approximately 200 wavenumbers each, small discontinuities appear in these spectra.

## Results

Rotation of the analyzer shows the nonresonant, resonant and combinations of the transmitted HIP-CARS signals, as shown in Fig. 3. The HIP-CARS lineshapes appear symmetric around the peaks and do not contain red-shifted peak and blue-shifted dip that are characteristic of isolated CARS responses. In practice, the nonresonant background is not completely removed. Birefringence in the sample, as well as polarization scrambling at the focus, leads to a slight depolarization of the CARS fields, and a small amount of the nonresonant component is interferometrically amplified. However, this amount is insignificant. A larger error is introduced by the small (several degrees) rotation of the polarization of the Stokes beam while scanning due to the dichroic mirrors. This alters the polarization of both the resonant and nonresonant beams, thus allowing more nonresonant background to pass the analyzer.

To demonstrate the background-free addressing of vibrational resonances in the fingerprint region, three spectra were recorded to compare hCARS, HIP-CARS, and spontaneous Raman from 600 to  $1650\text{ cm}^{-1}$ , see Fig. 4. The hCARS and HIP-CARS scans are both taken in five measurements of about 2 min each, at the maximum scan rate of the OPO, limited by the heating/cooling rate of the nonlinear periodically poled lithium niobate (PPLN) crystal.

Comparing HIP-CARS with the Raman spectra, it can be concluded that they are in good agreement over the full fingerprint region. This shows that HIP-CARS is an easy to use CARS technique to suppress the nonresonant background and obtain reliable vibrational information.

## Conclusion

We have shown that HIP-CARS is an effective technique to simultaneously extract and amplify the resonant component of a CARS spectrum. The HIP-CARS spectrum of toluene agrees well with the Raman spectrum, and none of the nonresonant effects that characterize CARS lineshapes are visible. We demonstrated this technique in a relatively unexplored fingerprint region, paving the way for further exploration of this region by background-free microscopy.

## References

- [1] P. D. Maker, R. W. Terhune, *Phys. Rev. Lett.* **1965**, *137*, A801.
- [2] T. Hellerer, C. Axang, C. Brackmann, P. Hillertz, M. Pilon, A. Enejder, *Proc. Natl. Acad. Sci. U.S.A.* **2007**, *104*, 14658.
- [3] M. Windbergs, M. Jurna, H. L. Offerhaus, J. L. Herek, P. Kleinebudde, C. J. Strachan, *Anal. Chem.* **2009**, *81*, 2085.

- [4] J. X. Cheng, X. S. Xie, *J. Phys. Chem. B* **2004**, *108*, 827.
- [5] A. Y. Chikishev, G. W. Lucassen, N. I. Koroteev, C. Otto, J. Greve, *Biophys. J.* **1992**, *63*, 976.
- [6] F. Ganikhanov, S. Carrasco, X. S. Xie, M. Katz, W. Seitz, D. Kopf, *Opt. Lett.* **2006**, *31*, 1292.
- [7] E. O. Potma, C. L. Evans, X. S. Xie, *Opt. Lett.* **2006**, *31*, 241.
- [8] M. Jurna, J. P. Korterik, C. Otto, J. L. Herek, H. L. Offerhaus, *Phys. Rev. Lett.* **2009**, *109*, 043905.
- [9] P. Nandakumar, A. Kovalev, A. Volkmer, *New J. Phys.* **2009**, *11*, 033026.
- [10] F. Lu, W. Zheng, Z. Huang, *Appl. Phys. Lett.* **2008**, *92*, 123901.
- [11] S. A. Akhmanov, A. F. Bunkin, S. G. Ivanov, N. I. Koroteev, *JETP Lett.* **1977**, *25*, 416.
- [12] J. Cheng, L. D. Book, X. S. Xie, *Opt. Lett.* **2001**, *24*, 1341.
- [13] M. Jurna, J. P. Korterik, C. Otto, J. L. Herek, H. L. Offerhaus, *Opt. Express* **2008**, *16*, 15863.
- [14] P. F. Chimento, M. Jurna, H. S. P. Bouwmans, E. T. Garbacik, L. Hartsuiker, C. Otto, J. L. Herek, H. L. Offerhaus, *J. Raman Spectrosc.* **2009**, *40*, 1229.
- [15] M. Jurna, J. P. Korterik, C. Otto, H. L. Offerhaus, *Opt. Express* **2007**, *15*, 15207.